# Controlling nanoscale optical emission with off-resonant laser light

David L. Andrews, Jamie M. Leeder and David S. Bradshaw
School of Chemistry, University of East Anglia, Norwich, NR4 7TJ, U.K.

In the optical excitation of many nanoscale systems, the primary result of photon absorption is an electronic excitation that is typically followed by ultrafast relaxation processes. The losses associated with such relaxation generally produce a partial degradation of the optical energy acquired, before any ensuing photon emission occurs. Recent work has shown that the intensity and directional character of such emission may be significantly influenced through engagement with a completely off-resonant probe laser beam of sufficient intensity: the mechanism for this optical coupling is a second-order nonlinearity. It is anticipated that the facility to actively control fluorescent emission in this way may lead to new opportunities in a variety of applications where molecular chromophores or quantum dots are used. In the latter connection it should prove possible to exploit the particle size dependence of the nonlinear optical dispersion, as well as that of the emission wavelength. Specific characteristics of the effect are calculated, and suitable experimental implementations of the mechanism are proposed. We anticipate that this all-optical control device may introduce significant new perspectives to fluorescence imaging techniques and other analytical applications.

**Keywords:** optical sensing, quantum dots, nonlinear optics, fluorescence imaging, nanophotonics, fluorophores

## 1. INTRODUCTION

In conventional molecular fluorescence, the characteristics of emission are relatively insensitive to the optical frequency of any monochromatic source used to create the initial electronic excitation. Obviously the input has to be encompassed by an absorption band of the material – and the frequency positioning of the input within the associated line-shape determines the strength of the excitation – but the rapid intramolecular relaxation processes that typically occur prior to fluorescence mean that the decay usually occurs from around the energy threshold of the electronically excited state, irrespective of the precise input frequency. Consequently, there is limited scope to explore dispersion properties of the material beyond the simple line-shape of the emission itself. In technical terms, the transition dipole moment for fluorescence emission is frequency-independent – at least, within the limits of validity of the usually applied Born-Oppenheimer approximation.

In a newly discovered process of optically controlled fluorescence, a passive beam engages with the emission through a third-order nonlinear response tensor that is indeed strongly dependent on optical frequency – in this sense, the transition moment for emission does acquire a frequency dependence. Consequently, there is a rich scope to explore and exploit the dispersion properties of the material through this optical nonlinearity; the mechanism affords a new parameter dimension for the analysis of fluorescence. In the present analysis, particular attention focuses on quantum dots, where there is additional scope to exploit a well-characterized size-dependence in the dispersion properties. The context for this focus is a wide recognition that these nanoparticles represent an attractive option as building blocks for photonic components, offering strong wavelength-selectable transitions and a high degree of photostability.[1] Amongst the wide-ranging investigations into such materials, a number of other recent studies have focused on Förster resonance energy transfer,[2-4] nonlinear optical response[5,6] and all-optical switching.[7,8]

## 2. LASER-MODIFIED FLUORESCENCE

Fluorescence, which occurs by spontaneous emission, generally involves a single matter-photon interaction as depicted in Fig. 1(a), and its standard theory is cast in terms of first-order time-dependent perturbation theory. When no other light is present – in particular, once any radiation responsible for the initial electronic excitation has passed out of the system, higher order (odd-rank) correction terms are insignificant and denote only self-energy corrections. However

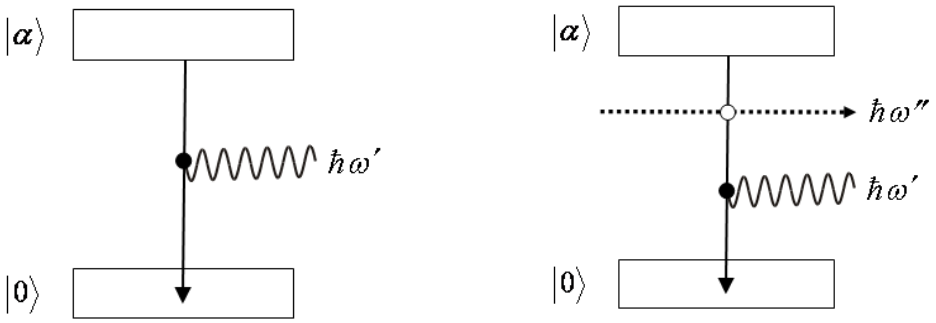


(a) (b)

Fig. 1. (a) Energy level representation for spontaneous fluorescence. Electronic states (and their vibrational manifolds) are signified by boxes, the wavy line is the emitted fluorescence ( $\hbar\omega'$ ) and the black vertical arrow is the decay transition: $|0\rangle$ and $|\alpha\rangle$ are the ground and excited states, respectively, the black dot symbolizing a single matter-photon interaction; (*b*) Same emission, but engaging an off-resonant laser beam ( $\hbar\omega''$ ) denoted by the horizontal dashed arrow; the open dot symbolizes two matter-photon interaction (i.e. elastic forward-scattering).

this is no longer the case when the fluorophore, in its electronic excited state, is subjected to a throughput of off-resonant laser light – the wavelength of the latter chosen to preclude stimulated emission or any excitation to higher electronic levels. Using a probe laser tuned to a region where the system is transparent, there can be no net absorption or stimulated emission, but elastic forward-scattering events do occur – photons are annihilated and created into the same radiation mode (which thus emerges unchanged). Such events can engage by nonlinear coupling with the fluorescence emission, and the effect is to modify the transition moment for fluorescence decay. This mechanism, represented in Fig. 1(b), entails three matter-photon interactions, i.e. third-order perturbation theory.

The intensity of fluorescence, $I'(\Omega')$ (power per unit solid angle), which follows from the Fermi Rule rate[9] multiplied by the energy of a fluorescence photon, $\hbar ck' \equiv \hbar\omega'$ ,[10] is now determined from $I'(\Omega') = 2\pi\rho ck' |M^{(1)} + M^{(3)}|^2$□, where $M^{(1)}$ and $M^{(3)}$ are the quantum amplitudes for the first- and third-order interaction processes, respectively, and the density of radiation states is $\rho = \left(k^2 V / 8\pi^3 \hbar c\right) \mathrm{d}\Omega$ .[11] The effects to be considered below depend on the relative signs of the first- and third-order amplitudes; a common sign leads to fluorescence enhancement, opposite signs its suppression. To proceed, the following is found for a given emission polarization;

$$I'(\Omega') = \left(\frac{ck'^4}{8\pi^2\varepsilon_0}\right)\Big[e'_i e'_j \mu_i^{0\alpha}\mu_j^{0\alpha} + (I/c\varepsilon_0)\, e'_i e''_j e''_k e'_l \chi_{ijk}^{0\alpha}(\omega';-\omega'',\omega'')\mu_l^{0\alpha} + \left(I^2/4c^2\varepsilon_0^2\right) e'_i e''_j e''_k e'_l e''_m e''_n \chi_{ijk}^{0\alpha}(\omega';-\omega'',\omega'')\chi_{lmn}^{0\alpha}(\omega';-\omega'',\omega'')\Big] \quad , \tag{1}$$

where $\chi_{ijk}^{0\alpha}$ is a transition hyperpolarizability tensor, $\mathbf{e}''$ and $\hbar\omega''$ correspond to the respective polarisation and energy of a probe laser photon, and *I* is the irradiance of the laser probe. Moreover, the implied summation convention for repeated Cartesian tensor indices is implemented. The initial term on the right-hand side in equation (1) corresponds to spontaneous emission – the usual one-photon transition, intrinsic to the system and independent of the probe laser beam – while the last term signifies a coupling of the elastically forward scattered probe beam with the fluorescence emission, a three-photon event. The second term, linear in *I*, represents a quantum interference of these two concurrent processes. In general, it may be assumed that the leading term in equation (1) is non-zero, and the second term a leading correction.

The relative sign of this correction will partly depend on the orientations of the relevant transition dipoles relative to the optical polarization vectors; one ensuing consequence of engagement with the probe beam is therefore a modification to the fluorescence anisotropy, an issue that has been discussed elsewhere. [12] Typically, assuming the relevant transition dipole components have broadly similar magnitudes and direction, it has also been determined that fluorescence can be expected to exhibit a change in intensity of ~ 10% for an irradiance of $10^{11}$ W cm$^{-2}$, and by ~ 50% for $I = 5 \times 10^{11}$ W cm$^{-2}$.

## 3. NON-RESONANT LIGHT AND QUANTUM DOT FLUORESCENCE

Amongst a diverse range of applications, quantum dots are exploited as highly efficient fluorophores, typically possessing excellent quantum yields and photostability as well as size-tunable and therefore highly selectable optical properties. The ease with which such systems can now be manufactured, chemically manipulated and structurally ordered, as well as their relative simplicity, also makes quantum dots the ideal prototype media in which to observe new nonlinear optical processes, such as the example outlined in Section 2, now investigated in the following analysis. To begin, the generalized form of the hyperpolarizability tensor $\chi_{ijk}^{0\alpha}\left(\omega';-\omega'',\omega''\right)$, as seen in equation (1), is defined as:

$$\begin{aligned}\chi_{ijk}^{0\alpha}\left(\omega';-\omega'',\omega''\right)=&\sum_{r}\sum_{s\neq\alpha}\left(\frac{\mu_i^{0s}\mu_j^{sr}\mu_k^{r\alpha}}{\tilde{E}_{s\alpha}\left(\tilde{E}_{r\alpha}-\hbar\omega''\right)}+\frac{\mu_i^{0s}\mu_k^{sr}\mu_j^{r\alpha}}{\tilde{E}_{s\alpha}\left(\tilde{E}_{r\alpha}+\hbar\omega''\right)}\right)\\&+\sum_{r}\sum_{s}\left(\frac{\mu_j^{0s}\mu_i^{sr}\mu_k^{r\alpha}}{\left(\tilde{E}_{s\alpha}-\hbar\omega''+\hbar\omega'\right)\left(\tilde{E}_{r\alpha}-\hbar\omega''\right)}+\frac{\mu_k^{0s}\mu_i^{sr}\mu_j^{r\alpha}}{\left(\tilde{E}_{s\alpha}+\hbar\omega''+\hbar\omega'\right)\left(\tilde{E}_{r\alpha}+\hbar\omega''\right)}\right)\\&+\sum_{r\neq 0}\sum_{s}\left(\frac{\mu_j^{0s}\mu_k^{sr}\mu_i^{r\alpha}}{\left(\tilde{E}_{s\alpha}-\hbar\omega''+\hbar\omega'\right)\left(\tilde{E}_{r\alpha}+\hbar\omega'\right)}+\frac{\mu_k^{0s}\mu_j^{sr}\mu_i^{r\alpha}}{\left(\tilde{E}_{s\alpha}+\hbar\omega''+\hbar\omega'\right)\left(\tilde{E}_{r\alpha}+\hbar\omega'\right)}\right),\end{aligned}\tag{2}$$

where $r$ and $s$ are intermediate matter states and $E_{xy}$ generally represents the energy difference between two possible molecular levels $x$ and $y$, i.e. $E_{xy} = E_x - E_y$. For simplicity, all photons in the following discussion are assumed to be linearly polarized. Each of the above transition moments is expressed with a concise short-hand where for example $\mu^{0r} = \langle 0|\mu|r\rangle$ – in which $|0\rangle$ denotes the ground matter state. Finally, the tildes serve as a reminder to add to the excited state energies, in the case of near-resonance conditions, imaginary terms that accommodate damping.

Considering the dependence of the fluorescence signal on the optical frequency of the probe beam, it is evident that the denominators within the susceptibility of equation (2) are the primary factors determining the degree of enhancement or suppression of the fluorescence emission. These factors are ultimately determined by the relative positioning of the fluorophore energy levels, relative to the magnitude of the probe photon energy. To discover more, we focus on the common case where the initially activated level $|\alpha\rangle$ is the lowest accessible electronic excited state. Consequently, it is convenient to assume that the probe light is delivered with a tunable beam of frequency $\omega'' < \omega'$, specifically precluding excitation to any higher electronic levels from the ground state. The main challenge in evaluating the nonlinear response characterized by the hyperpolarizability tensors within equation (1) now lies with implementing the required sum over all intermediate states. There is a potentially infinite number of energy levels associated with both $r$ and $s$, and to ease calculational complexity it is common to reduce such sets to a small finite number by approximation. In the present context, it is defensible to consider only the states through which the majority of the optical transitions occur, which in

the case of many fluorescence systems limits the choice to just the ground and lowest energy excited states, i.e. a two-state approximation. Such an approach is particularly apposite for quantum dot systems.

Restricting both intermediate states featured within equation (2) to just $|0\rangle$ and $|\alpha\rangle$, only four unique routes of levels exist that can describe transition from the excited to ground matter states progressing through both *r* and *s* – the $\alpha \to r \to s \to 0$ sequences specifically expressible as $\alpha 000$, $\alpha\alpha 00$, $\alpha 0\alpha 0$ and $\alpha\alpha\alpha 0$. Each sequence generates a combination of both transition dipole moments, either $\boldsymbol{\mu}^{0\alpha}$ or $\boldsymbol{\mu}^{\alpha 0}$, as well as the static dipole moments of the ground and excited energy levels, $\boldsymbol{\mu}^{00}$ and $\boldsymbol{\mu}^{\alpha\alpha}$ respectively. Detailed analysis of nonlinear optical susceptibilities shows that the dependence on static moments emerges only in terms of their vector difference, $\boldsymbol{d} = \boldsymbol{\mu}^{\alpha\alpha} - \boldsymbol{\mu}^{00}$, and with the benefit of an algorithmic method, the following prescription can be adopted:[13]

$$\boldsymbol{\mu}^{\alpha\alpha} \to \boldsymbol{\mu}^{\alpha\alpha} - \boldsymbol{\mu}^{00} = \boldsymbol{d} \;;\; \boldsymbol{\mu}^{00} \to 0. \tag{3}$$

Applying this protocol requires application of an associated rule: any transitional mechanism that connects the initial and final system states through any ground state static dipole is to be discarded, and hence only two of the originally proposed four sequences, namely $\alpha 0\alpha 0$ and $\alpha\alpha\alpha 0$ persist. Applied to the six terms within equation (2), each of which represents a unique time-ordering of the nonlinear process, the two-level hyperpolarizability tensor is generally expressible as a sum of 12 separate contributions. Further simplification ensues because a number of these terms, when $r = 0$ and/or $s = \alpha$, are precluded by the conditions of perturbation theory. The two-state form of $\chi_{ijk}^{0\alpha}(\omega'; -\omega'', \omega'')$ is subsequently reinterpreted as:

$$\chi_{ijk}^{0\alpha}(\omega'; -\omega'', \omega'') = 2\left(\frac{\mu_j^{0\alpha}\mu_i^{\alpha 0}\mu_k^{0\alpha}}{(\hbar\omega'' + \hbar\omega')(\hbar\omega'' - \hbar\omega')}\right) + \mu_j^{0\alpha} d_i\, d_k \left(\frac{1}{(\hbar\omega'')^2 - \hbar\omega''\hbar\omega'} + \frac{1}{(\hbar\omega')^2 - \hbar\omega''\hbar\omega'}\right)$$
$$+ \mu_k^{0\alpha} d_i\, d_j \left(\frac{1}{(\hbar\omega'')^2 + \hbar\omega''\hbar\omega'} + \frac{1}{(\hbar\omega')^2 + \hbar\omega''\hbar\omega'}\right) . \tag{4}$$

The form of equation (4) can be yet further simplified by considering the effects of index symmetry. The nonlinear contribution of equation (1) being fully symmetric in the *j* and *k* indices of the electric polarization vectors, allows equation (4) to be defined in terms of the partially symmetric polarizability tensor $\chi_{i(jk)}^{0\alpha}(\omega'; -\omega'', \omega'')$ such that:

$$\chi_{i(jk)}^{0\alpha}(\omega'; -\omega'', \omega'') \equiv \frac{1}{2}\left(\chi_{ijk}^{0\alpha}(\omega'; -\omega'', \omega'') + \chi_{ikj}^{0\alpha}(\omega'; -\omega'', \omega'')\right) = 2\frac{\mu_j^{0\alpha}\mu_i^{\alpha 0}\mu_k^{0\alpha}}{(\hbar\omega'' + E_{\alpha 0})(\hbar\omega'' - E_{\alpha 0})} . \tag{5}$$

The above expression has been cast relative to the energy difference between the ground and excited states through the relationship $E_{\alpha 0} = \hbar\omega'$. Exploiting a unique property of quantum dots, the same energy difference is itself dependent on particle size through the following expression:[14]

$$E_{\alpha 0} = E_{\alpha 0}^0 + K\left(R^{-2}\right), \tag{6}$$

where $E_{\alpha 0}^0$ represents the difference in energy between excited and ground states of the bulk semi-conductor material i.e. on scales outside the quantum size regime, where the energy gap becomes insensitive to particle size. The second term in equation (6) represents a correction term highlighting the well-known blue-shift in emission wavelength with decreasing quantum dot radius, *R*. The constant *K* is expressible as:

$$K = \hbar^2 \pi^2 \left(2m_{eh}\right)^{-1} , \tag{7}$$

with $m_{eh}$ the reduced mass of the electron-hole pair. By substitution of equation (6) into the right hand side of equation (5):

$$\chi^{0\alpha}_{i(jk)}\left(\omega';-\omega'',\omega''\right) = 2\mu_j^{0\alpha}\mu_i^{\alpha 0}\mu_k^{0\alpha}\left[\left(\hbar\omega''\right)^2 - \left(E^0_{\alpha 0}\right)^2 - 2KE^0_{\alpha 0}\left(R^{-2}\right) - K^2\left(R^{-4}\right)\right]^{-1} . \tag{8}$$

As a correction term, it can generally be assumed that $K\left(R^{-2}\right)$ is small in comparison to both $\left(\hbar\omega'' + E^0_{\alpha 0}\right)$ and $\left(\hbar\omega'' - E^0_{\alpha 0}\right)$, and therefore by extension, the $K^2\left(R^{-4}\right)$ term within equation (8) represents an insignificant contribution that is subsequently discarded. Moreover, with a Taylor series expansion the two-state hyperpolarizability tensor can be presented in a final form as:

$$\chi^{0\alpha}_{i(jk)}\left(\omega';-\omega'',\omega''\right) = 2\mu_j^{0\alpha}\mu_i^{\alpha 0}\mu_k^{0\alpha}\left(\frac{1}{\left(\hbar\omega''\right)^2 - \left(E^0_{\alpha 0}\right)^2} + \frac{2KE^0_{\alpha 0}\left(R^{-2}\right)}{\left(\left(\hbar\omega''\right)^2 - \left(E^0_{\alpha 0}\right)^2\right)^2}\right). \tag{9}$$

Essentially, the first term in equation (9) represents the nonlinear response to any bulk material undergoing fluorescence decay, whilst subject to an input of non-resonant light; the second term is characteristic of quantum dots of a particular size.

## 4. DIRECTED FLUORESCENCE

We now consider, in detail, the spatial characteristics of the fluorescence emerging from a sample whose emission is subjected to the laser modification described in the previous Section. It is supposed that the fluorescence is detected by a probe device, sensitive to the emission wavelength, whose variable positioning is employed to analyse the directionality of the emission. It transpires that the emission field of any excited fluorophore is modified, and the transportation of electronic excitation energy from the fluorophore to the probe is augmented. Over typical sample-probe distances this energy transportation takes the form of radiant fluorescence and subsequent absorption; however in the near-field, i.e. over sub-wavelength distances, a modified form of resonance energy transfer (RET) dominates; the latter is our present concern. For arbitrary positions of the probe, relative to the fluorophore source, the power, $P'$, acquired by the detector (hence the signal strength) is again determined from the Fermi rule, namely;

$$P' = 2\pi\omega'\rho\left|M^{(2)} + M^{(4)}\right|^2 \quad . \tag{10}$$

where $M^{(2)}$ and $M^{(4)}$ are the quantum amplitudes for second- and fourth-order interaction processes, respectively; both terms are one interaction order larger than those presented earlier, since the theory now accommodates an additional photon detection event at the probe. Specifically, $M^{(2)}$ corresponds to the second-order coupling of conventional (laser throughput-independent) RET, whilst the contribution $M^{(4)}$ represents the optically nonlinear influence of the input beam. In more detail, $M^{(4)}$ involves two mechanistic components; laser photon absorption at source *A*, stimulated emission at probe *B*, and the converse. Accounting for each of the routes for the detector to register a signal, the complete derivation of $M^{(4)}$, as delivered by previous work,[15] yields the following;

$$M^{(4)} = \left( \frac{(I_A I_B)^{\frac{1}{2}}}{8\pi\varepsilon_0^2 c R^3} \right) e_i e_l \left( \delta_{jk} - 3\hat{R}_j \hat{R}_k \right) \left( \chi_{ij}^A(\omega)\chi_{lk}^B(-\omega) + \chi_{ij}^B(\omega)\chi_{lk}^A(-\omega) \right) \ , \tag{11}$$

where $R = |\mathbf{R}|$ is the magnitude of the source-probe separation vector, $I_\xi$ is the irradiance of the input Gaussian beam at the position of molecule $\xi$. Taking (10), and the commonly known equation of RET (i.e. $M^{(2)}$),[16] an intricate general expression can be determined for the detected power $P'$, as is quoted in full elsewhere.[17]

Now a configuration is chosen so that the throughput beam propagates in the *z*-direction, perpendicular to the plane in which the probe moves, and centered upon the position of closest approach, i.e. the origin in the (*x*, *y*) plane (Fig. 2). Thus, through deploying this configuration, the following result arises:

$$P' = \frac{\omega' \mu^4 \rho}{8\pi\varepsilon_0^2 \left( r^2 + z^2 \right)^5} \left\{ \frac{(I_A I_B)^{\frac{1}{2}} \mu^2 \left( r^2 - 2z^2 \right)}{4c\varepsilon_0 \Delta E^2} - 3xy \right\}^2 \ . \tag{12}$$

Here, $\mu$ is the magnitude of the transition dipole moment for the source and probe – although, for these calculations, $\boldsymbol{\mu}^A$ and $\boldsymbol{\mu}^B$ are assumed to be directed in the $\hat{\mathbf{i}}$ and $\hat{\mathbf{j}}$ directions, respectively – *r* is the magnitude of the projection of particle-probe separation vector, **R**, on the *x*, *y*-plane. Moreover, $\Delta E$ is a finite energy which is significantly lower in magnitude than a typical transition energy (explicitly defined elsewhere).[17] The mappings shown in Figs 3(a)-(d) portray $P'/\kappa$ – where $\kappa = \omega\mu^4\rho/8\pi\varepsilon_0^2$ – as a function of *x* and *y* for different values of $I_0$; the latter denotes the laser irradiance at the beam centre (the associated Gaussian profile being determined by $I_\xi = I_0 \mathrm{e}^{-2(r/w)^2}$, where 2*w* defines the beam waist). The values $\Delta E = 5 \times 10^{-20}$ J and $w = 500$ nm are used in creation of the contour maps. The graphs signify that the shape of the near-field distribution becomes significantly distorted with a sufficient level of input beam irradiance. On introduction of an increasingly powerful off-resonant beam, the four lobes of the conventional cross-polarized fields

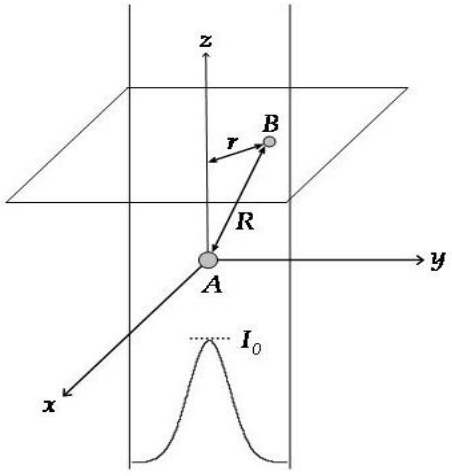


Fig. 2. Geometry of configuration described in text, indicating that the source *A* and detector *B* are encompassed within the Gaussian profile of a throughput laser beam propagating along the *z*-axis.

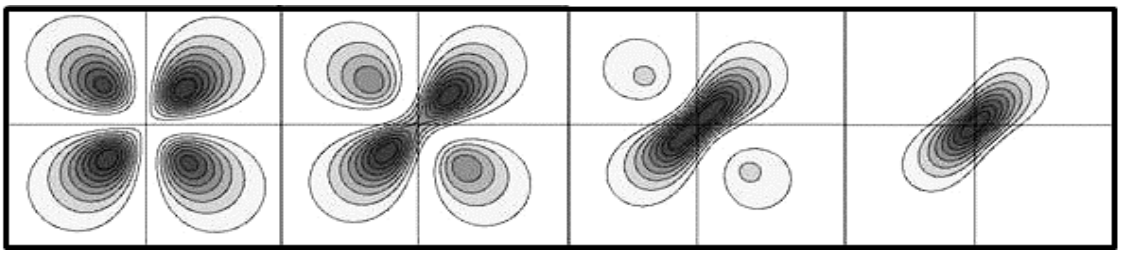

(a) (b) (c) (d)

Fig. 3. Contour maps of $P'/K$ against $x$ and $y$ (both in nm) with $z$ = 40 nm, cross-polarized configuration (see text). The input laser irradiance at the beam center, $I_0$, is: (a) $3\times10^{11}$ W cm$^{-2}$, (b) $1\times10^{12}$ W cm$^{-2}$, (c) $2\times10^{12}$ W cm$^{-2}$, and (d) $3\times10^{12}$ W cm$^{-2}$.

begin to coalesce and, with increasing $I_0$, they eventually merge and compress into a single circular peak centred on the origin. Intermediate stages between the two extremes are shown in Fig. 3: (a) $I_0 = 3 \times 10^{11}$ W cm$^{-2}$, two diagonally opposite peaks first show convergence towards the origin; (b) $1 \times 10^{12}$ W cm$^{-2}$, the same peaks begin to merge and the other maxima decrease in magnitude; (c) $2 \times 10^{12}$ W cm$^{-2}$, the two major peaks fully coalesce and other maxima become diminutive; (d) $3 \times 10^{12}$ W cm$^{-2}$, the distribution resolves into one elliptical peak at the origin. At higher intensities this peak becomes increasingly circular.

## 5. DISCUSSION

The capacity to optically control emission represents the addition of another dimension to the parameter space for fluorescence experimentation. In particular, since the mechanism for this control involves an optical nonlinearity of distinctive dispersion form, it affords a potential means of discrimination between chemically distinct sources of emission. In the fluorescence analysis and imaging of complex multichromophore media, there are certainly opportunities to increase the quantity of deliverable information, especially when intense fluorophores have significantly overlapping spectra. Moreover, the anticipated enhanced directionality of the fluorescence emission suits near-field imaging. The general analysis presented in this paper provides all that is needed to interpret observations.

The development of theory for application to quantum dots is relevant for a potentially very different kind of system. The characteristic size-determined emission wavelength of such nanoparticles, when based as extrinsic reporter fluorophores, generally obviates the need for any further, optically-assisted methods of site differentiation. However, a monodisperse sample of quantum dots, deployed as a source of monochromatic emission under conventional illumination, offers other opportunities for exploiting control by off-resonant light. The ultrafast response to the latter input, used to trigger fluorescence emission, suggests a variety of switching applications. It is notable that the specific optical nonlinearity at the heart of the mechanism – the tensor $\chi$ defined in equation (2) in the present analysis – proves to deliver a signal that depends only on the transition dipole moment, in the two-state approximation. This contrasts with more common forms of two-level optical nonlinearities that engage *two* electrical parameters – the transition dipole moment, and the difference in static dipoles between the ground and excited states.[13] In consequence, the operation of optically controlled fluorescence in quantum dot systems is not crucially dependent on structural anisotropy; it should be observable in all the commonly studied varieties of quantum dots. It is also interesting to observe that the extent of optical control – quantified as the degree of response to the control radiation – is itself functionally dependent on particle size. This dependence is not critical; as equation (9) shows, the dominant term in the response is not size-dependent.

## ACKNOWLEDGEMENTS

The authors are grateful to both EPSRC (JML) and the Leverhulme Trust (DSB) for financial support, and for funding this research. We also thank Prof. Thomas Nann for an insightful discussion.

## REFERENCES


[1] Prasad, P. N., [Nanophotonics], Wiley, Hoboken, NJ (2004).

[2] Curutchet, C., Franceschetti, A., Zunger A. and Scholes, G. D., "Examining Förster energy transfer for semiconductor nanocrystalline quantum dot donors and acceptors," J. Phys. Chem. C 112, 13336-13341 (2008).

[3] Lunz, M., Bradley, A. L., Chen, W.-Y. and Gun'ko, Y. K., "Förster resonant energy transfer in quantum dot layers," J. Phys. Chem. C 113, 3084-3088 (2009).

[4] Sun, Z., Juriani, A., Meininger, G. A. and Meissner, K. E., "Probing cell surface interactions using atomic force microscope cantilevers functionalized for quantum dot-enabled Förster resonance energy transfer," J. Biomed. Opt. 14, 040502 (2009).

[5] Guenther, T., Lienau, C., Elsaesser, T., Glanemann, M., Axt, V. M., Kuhn, T., Eshlaghi, S. and Wieck, A. D., "Coherent nonlinear optical response of single quantum dots studied by ultrafast near-field spectroscopy," Phys. Rev. Lett. 89, 057401 (2002).

[6] Wesseli, M., Ruppert, C., Trumm, S., Krenner, H. J., Finley, J. J. and Betz, M., "Nonlinear optical response of a single self-assembled InGaAs quantum dot: A femtojoule pump-probe experiment," Appl. Phys. Lett. 88, 203110 (2006).

[7] Prasanth, R., Haverkort, J. E. M., Deepthy, A., Bogaart, E. W., van der Tol, J. J. G. M., Patent, E. A., Zhao, G., Gong, Q., van Veldhoven, P. J., Nötzel, R. and Wolter, J. H., "All-optical switching due to state filling in quantum dots," Appl. Phys. Lett. 84, 4059-4061 (2004).

[8] Bradshaw, D. S. and Andrews, D. L., "All-optical switching between quantum dot nanoarrays," Superlatt. Microstruct. 47, 308-313 (2010).

[9] Mandel, L. and Wolf, E., [Optical Coherence and Quantum Optics], University Press, Cambridge, 871 (1995).

[10] Andrews, D. L. and Allcock, P., [Optical Harmonics in Molecular Systems], Wiley-VCH, Weinheim (2002).

[11] Craig, D. P. and Thirunamachandran, T., [Molecular Quantum Electrodynamics], Dover, New York (1998).

[12] Bradshaw, D. S. and Andrews, D. L., "Mechanism for optical enhancement and suppression of fluorescence," J. Phys. Chem. A 113, 6537-6539 (2009).

[13] Andrews, D. L., Dávila Romero, L. C. and Meath, W. J., "An algorithm for the nonlinear optical susceptibilities of dipolar molecules, and an application to third harmonic generation," J. Phys. B: Atom. Molec. Opt. Phys. 32, 1-17 (1999).

[14] Klimov, V. I., "Nanocrystal quantum dots: From fundamental photophysics to multicolor lasing," Los Alamos Science 28, 214-220 (2003).

[15] Bradshaw, D. S. and Andrews, D. L., "The control of near-field optics: imposing direction through coupling with off-resonant laser light," Appl. Phys. B 93, 13-20 (2008).

[16] Juzeliūnas, G. and Andrews, D. L., [Resonance Energy Transfer], Wiley, Chichester, chapter 2 (1999).

[17] Bradshaw, D. S. and Andrews, D. L., "Optically controlled resonance energy transfer: Mechanism and configuration for all-optical switching," J. Chem. Phys. 128, 144506 (2008).